Anti-inflammatory components isolated from Atractylodes macrocephala in LPS-induced RAW264.7 macrophages and BV2 microglia

Hong-Quang Jin
Jiujiang University
Kwan-Woo Kim
Rural Development Administration
Jing Li
Wonkwang University
Dae Young Lee
Rural Development Administration
Dahye Yoon
Rural Development Administration
Jin Tae Jeong
Rural Development Administration
Geum-Soog Kim
Rural Development Administration
Hyuncheol Oh
Wonkwang University
Ren-Bo An
Yanbian University
Youn-Chul Kim (yckim@wku.ac.kr)
Wonkwang University https://orcid.org/0000-0002-1458-9536

Research Article

Keywords: Atractylodes macrocephala, anti-inflammatory effect, macrophages, microglia, nuclear factor kappa B

Posted Date: April 22nd, 2021

DOI: https://doi.org/10.21203/rs.3.rs-429158/v1

Abstract

The phytochemical investigation on the methanol extract of the rhizomes of *Atractylodes macrocephala* resulted in the discovery of one new compound 9α-hydroxyatractylenolide (**1**) and 21 known compounds including atractylone (**2**), 3β-acetoxyatractylon (**3**), atractylenolide I (**4**), atractylenolide II (**5**), 8-epiasterolid (**6**), atractylenolide III (**7**), atractylenolide VII (**8**), 8-epiatractylenolide III (**9**), eudesm-4(15)-ene-7α,11-diol (**10**), linoleic acid (**11**), myristic acid (**12**), 3-*O*-caffeoyl-1-methyquinic acid (**13**), (2E,8E,10E)-tetradecatriene-4,6-diyne-1,14-diol (**14**), 14-aceroxy-12-senecioyloxytetradeca-2E,8Z,10E-trien-4,6-diyn-1-ol (**15**), isoscopoletin (**16**), caffeic acid (**17**), protocatechic acid (**18**), 3-*O*-caffeoylquinic acid (**19**), 4-*O*-caffeoylquinic acid (**20**), 1,5-di-*O*-caffeoylquinic acid (**21**), and nicotinic acid (**22**). Their structures were identified using nuclear magnetic resonance (NMR) and mass spectroscopy, and by comparison with previously published data. Compounds **4**, **5**, **6**, **8**, and **10**–**22** significantly inhibited lipopolysaccharide (LPS)-induced nitric oxide (NO) production in RAW264.7 macrophages, and compounds **4**, **5**, **6**, **16**, and **17** showed those responses in BV2 microglial cells. Especially, compound **6** showed the second-best effect, and inhibited the LPS-induced production of prostaglandin E2 (PGE_2), the protein expression of inducible nitric oxide synthase (iNOS) and cyclooxygenase (COX)-2, and the production of cytokines including interleukin (IL)-1β, IL-6, and tumor necrosis factor (TNF)-α in both cells. These inhibitory effects were mediated by the inactivation of nuclear factor kappa B (NF-κB) signaling pathway.

Introduction

Inflammation is associated with the activation of macrophages or monocytes that are responsible for the innate and adaptive immune responses of the human body. Following various stimuli, these immune cells release a series of pro-inflammatory mediators including nitric oxide (NO), prostaglandin E2 (PGE_2), cytokines such as interleukin (IL)-1β, IL-6, and tumor necrosis factor (TNF)-α, chemokines, and signaling-associated proteins [1] to protect the infected tissues site and to maintain the homeostasis of the body [2]. However, a dysregulation of the inflammatory responses via continuous stimulation results in the overproduction of pro-inflammatory mediators, leading to the development of various inflammatory diseases including atherosclerosis, cardiovascular disorders, diabetes, tumor, asthma, septic complications, and neurodegenerative diseases [3-5]. Macrophages are the most dominant and widely distributed immune cell types throughout the body, and microglia are considered resident macrophages in the central nervous system (CNS) [6]. Macrophages and microglia are important sources of pro-inflammatory mediators through the activation of transcription factors such as nuclear factor kappa-light-chain-enhancer of activated B cells (NF-κB) and mitogen-activated protein kinase (MAPK) due to lipopolysaccharide (LPS) stimulation [7, 8]. LPS is the most abundant lipidic component of the gram-negative bacterial cell wall [9]. Since macrophages and microglia stimulated by LPS produce excessive pro-inflammatory mediators, they are being utilized in in vitro models to evaluate the effectiveness of potentially anti-inflammatory candidate substances [10, 11].

Atractylodes macrocephala, which belongs to the Compositae family, is a perennial herb, widely distributed in East Asia [12]. Traditionally, this plant has been used for the treatment of an abnormal

function of the digestive system including malfunction of the spleen, anorexia, abdominal distension, diarrhea, dizziness, and palpitation due to the retention of phlegm and fluid, edema, spontaneous sweating, threatened abortion, oedema, excessive perspiration, and an abnormal fetal movement [13, 14]. In several recent studies, various components of *A. macrocephala* were isolated including essential oils, sesquiterpenoids, polysaccharides, amino acids, vitamins, and resins [15], and their physiological activity including anti-inflammatory [16], neuroprotective [17], anti-cancer [18], anti-oxidant [19], and immunological enhancement effects [20] were evaluated. In this investigation, we described the isolation and structural identification of 22 compounds from the rhizomes of *A. macrocephala* together with the evaluation of their anti-inflammatory effects using RAW264.7 macrophage and BV2 microglial cell lines.

Materials And Methods

Plant materials

The rhizomes of *A. macrocephala* were harvested in Andong (Gyeongbuk) in December 2018. The plant material was identified by Prof. Youn-Chul Kim, College of Pharmacy, Wonkwang University, Iksan, Korea. A specimen of *A. macrocephala* (no. WSY-2019-003) has been deposited at the College of Pharmacy, Wonkwang University, Korea.

Extraction and Isolation

The dried rhizomes of *A. macrocephala* (2.0 kg) were cut and extracted using MeOH three times for 3 h at 80 °C. The resultant MeOH extract (100.9 g) was suspended in water (1.0 L×3) and then sequentially partitioned using equal volumes of n-hexane, dichloromethane, ethyl acetate, and n-butanol. Each fraction was evaporated in vacuo to yield the residues of n-hexane (8.9 g), CH_2Cl_2 (3.7 g), EtOAc (1.5 g), n-BuOH (3.9 g), and water (72.3 g) extracts, respectively.

The n-hexane soluble fraction (8.5 g) was subjected to column chromatography (CC) using a silica gel column and eluted with an n-hexane/EtOAc (100:0→1:1) gradient system. The fractions were combined based on their thin layer chromatography (TLC) pattern to yield subfractions, which were designated H1-H7. Fraction H1 (3.8 g) was purified by Sephadex LH-20 CC (n-hexane, 100:0) to yield six subfractions (H11-H16). Subfraction H11, containing **2** was purified by silica gel CC (n-hexane/EtOAc, 100:1→10:1), and by ODS CC (MeOH/H_2O, 1:1→2:1) to yield **2** (212.6 mg). In addition, subfraction H13 was purified by silica gel CC (n-hexane/EtOAc, 30:1→10:1), and by ODS CC (MeOH/H2O, 1:1→3:1) to yield **9** (12.0 mg) and **5** (90.2 mg). Subfraction H15 was purified by silica gel CC (n-hexane/EtOAc, 20:1→5:1), and by ODS CC (MeOH/H_2O, 1:1→2:1) to yield **6** (2.6 mg). Fraction H2 (1.1 g) was subjected to silica gel CC eluting with an n-hexane/EtOAc (50:1→10:1) gradient system to yield three subfractions (H21-H23). Subfraction H21 was then purified by repeated ODS CC (MeOH/H_2O, 2.5:1→3.5:1) to yield **3** (13.2 mg), and **8** (50.6 mg). Fraction H3 (1.2 g) was subjected to silica gel CC eluting with a n-hexane/EtOAc (15:1→5:1) gradient system to yield six subfractions (H31-H36). Subfraction H31 was purified by silica gel CC (n-hexane/EtOAc, 25:1→15:1), and by ODS CC (MeOH/H_2O, 1.5:1→3.5:1) to yield **4** (55.6 mg) and **7** (165.6

mg). Moreover, subfraction H34 was then purified by ODS CC (MeOH/H_2O, 4.5:1→6:1) to yield **11** (73.2 mg), and **12** (23.0 mg). Fraction H4 (435.2 mg) was subjected to silica gel CC eluting with a n-hexane/EtOAc (8:1→4:1) gradient system to achieve five subfractions (H41-H45). Subfraction H42 was purified by ODS CC (MeOH/H_2O, 1.5:1→3:1) to yield **10** (13.2 mg).

The CH_2Cl_2 soluble fraction (3.5 g) was subjected to CC using a Sephadex LH 20 column and eluted with CH_2Cl_2/MeOH (1:1 and 100%MeOH) system. The fractions were combined based on their TLC pattern to yield subfractions, which were designated D1-D4. Fraction D2 (596.8 mg) was subjected to silica gel CC eluting with n-hexane/EtOAc (5:1→1:1) gradient system to yield eight subfractions (D21-D28). Subfraction D25 was purified by ODS CC (MeOH/H_2O, 1:1→2:1), followed by preparative high-performance liquid chromatography (HPLC) eluted with MeOH/H2O (60:40) to give **14** (12.4 mg). Fraction D3 (464.6 g), containing **15**, and **16** was purified by silica gel CC n-hexane/EtOAc (4:1→1:1), followed by medium pressure liquid chromatography (MPLC) (MeOH/H_2O, 3:1→1:1), and finally by ODS CC (MeOH/H_2O, 2:1→1:1) to give **15** (33.2 mg) and **16** (11.2 mg).

The EtOAc soluble fraction (1.1 g) was subjected to CC using a silica gel column and eluted with $CHCl_3$/MeOH/H_2O (20:1:0.1→1:1:0.1) gradient system. The fractions were combined based on their TLC pattern to yield subfractions, which were designated E1-E10. Fraction E3 (135.7 mg) was subjected to ODS CC eluting with MeOH/H_2O (3:1→1.5:1) gradient system to give six subfractions (E31-E36). Subfraction E33 was purified by silica gel CC ($CHCl_3$/MeOH, 9:1) to give **12** (32.2 mg). Fraction E5 (359.2 mg) was subjected to silica gel CC eluting with a $CHCl_3$/MeOH/H_2O (4:1:0.1→1:1:0.1) gradient system to give six subfractions (E51-E56). Subfraction E53 was purified by MPLC (MeOH/H_2O, 1:4→1:3), and by ODS CC (MeOH/H_2O, 1:3.5) to give **17** (8.3 mg) and **18** (6.0 mg). Fraction E8 (204.5 mg) was subjected to silica gel CC eluting with $CHCl_3$/MeOH/H_2O (3:1:0.1→ 1:1:0.1) gradient system to give eight subfractions (E81-E88). Subfraction E85 was purified by ODS CC (MeOH/H_2O, 1:2→1:1), followed by preparative HPLC eluting with MeOH/H_2O (20:80→60:40) gradient system, to give **19** (10.6 mg), **20** (2.6 mg), and **21** (9.8 mg). Besides, subfraction E87 was purified by ODS CC (MeOH/H2O, 1:1.5) to give **22** (14.5 mg).

Chemicals and reagents

Tissue culture reagents RPMI1640, Dulbecco's modified Eagle's medium (DMEM) and fetal bovine serum (FBS) were obtained from Gibco BRL Co. (Grand Island, NY, USA). LPS was purchased from Sigma-Aldrich (St. Louis, MO, USA). 3-[4,5-dimethylthiazol-2-yl]-2, 5-diphenyltetrazolium bromide sodium (MTT) was obtained from Glentham Life Sciences (Corsham, UK). The anti-inducible nitric oxide synthase (iNOS) primary antibodies were purchased from Cayman (Ann Arbor, MI, USA), anti-cyclooxygenase (COX)-2, anti-inhibitor kappa B (IκB)-a, anti-p-IκB-a, anti-p-p65, anti-p65, anti-p-extracellular signal-regulated kinase (ERK), anti-ERK, anti-p-c-Jun N-terminal kinase (JNK), anti-JNK, anti-p-p38, and anti-p38 from Cell Signaling (Danvers, MA), and anti-β-actin from Santa Cruz Biotechnology (Dallas, TX, USA), respectively. Anti-mouse, anti-goat, and anti-rabbit secondary antibodies were purchased from Merck Millipore (Darmstadt, Germany).

Cell culture

The immortalized murine RAW264.7 macrophages and BV2 microglial cells were maintained at 5×10^5 cells/mL in 100 mm dishes in RPMI1640 medium supplemented with 10% (v/v) heat-inactivated FBS, penicillin G (100 units/mL), streptomycin (100 mg/mL), and L-glutamine (2 mM), and cultured at 37 °C in a humidified atmosphere containing 5% CO_2.

Cell viability assay

An MTT assay was conducted to determine cell viability. RAW264.7 and BV2 cells were cultured in a 96-well plate at a density 1×10^5 cell/mL, and the cultured cells were treated with the test compounds for 24 h. Subsequently, 50 µL of an MTT solution were added to each well at a final concentration of 0.5 mg/mL, and the cells were incubated for 3 h in a humidified incubator at 37 °C. After removing the supernatant, the formazan formed was dissolved in 150 µL of dimethyl sulfoxide (DMSO), and mixed for 15 min. The optical density of the DMSO solution was measured at 540 nm wavelength using a microplate reader (Bio-Rad, Hercules, CA, USA). The optical density of the formazan formed in the control (untreated group) cells was considered to represent 100% viability, and the viability of cells in other groups was expressed as a percentage of obtained viable cells relative to the control. This assay was independently conducted three times.

Determination of nitrite

Nitrite is an indicator of NO production; its concentration in the culture medium was measured using the Griess reaction. RAW264.7 and BV2 cells were cultured in a 24-well plate at a density of 2×10^5 cell/mL for 12 h. Cells were treated with test compounds for 3 h, and then stimulated with LPS (1 µg/mL) for 24 h. Each culture medium (100 µL) was mixed with the same volume of Griess reagent (Sigma-Aldrich, St. Louis, MO, USA) for 15 min at room temperature. The absorbance was measured spectrophotometrically at 540 nm wavelength using an enzyme-linked immunosorbent assay (ELISA) plate reader. The nitrite concentration in the culture medium was determined from a standard curve of sodium nitrite.

PGE_2 assay

The culture media were collected to determine the PGE_2 level present in each sample using the appropriate ELISA kit from ENZO Life Sciences (Farmingdale, NY, USA). Three independent assays were performed according to the manufacturer’s instructions.

IL-1β, IL-6, and TNF-α assays

The levels of IL-1β, IL-6, and TNF-α present in each sample were determined using a commercially appropriate kit from R&D Systems (Minneapolis, MN). Three independent assays were performed according to the manufacturer's instructions.

Western blot analysis

RAW264.7 and BV2 cells were cultured in a 6-well plate at a density of 2×10^5 cell/mL for 12 h. Then cells were treated with the test compounds for 3 h, followed by stimulation with LPS (1 μg/mL) for 24 h. Radioimmunoprecipitation assay (RIPA) buffer (Thermo Scientific, MA, USA) was used to prepare lysate. The concentration of protein was measured using Bradford protein assay (Bio-Rad Laboratories, CA, USA) and normalized to ensure that equal amounts were loaded. Subsequently, 30 μg of protein from each sample were resolved using 6%, 8%, and 12% sodium dodecyl sulfate-polyacrylamide gel electrophoresis (SDS-PAGE). The proteins were electrophoretically transferred onto Hybond enhanced chemiluminescence (ECL) nitrocellulose membranes (Bio-Rad, Hercules, CA, USA). The membranes were blocked with 5% skim milk and sequentially incubated with particular primary antibodies and horseradish peroxidase (HRP)-conjugated secondary antibodies, followed by ECL detection (Amersham Pharmacia Biotech, Piscataway, NJ, USA).

Statistical analysis

The data are expressed as mean ± standard deviation (SD) of at least three independent experiments. To compare three or more groups, a one-way analysis of variance (ANOVA) was used, followed by Tukey's multiple comparison tests. Statistical analysis was performed using GraphPad Prism software, version 3.03 (GraphPad Software Inc., San Diego, CA, USA).

Results And Discussion

Compounds isolated from *A. macrocephala*

Twenty-two compounds were isolated from the rhizomes of A. macrocephala using various combined chromatographic methods. The nuclear magnetic resonance (NMR) and mass spectroscopy (MS) data of the isolated compounds were analyzed and compared with those reported in the literature to elucidate the structures of the isolated compounds. Compound **1** was obtained as a white solid. $[\alpha]_D^{23}$ + 232.4 (c 0.07, MeOH). Its molecular formula of $C_{15}H_{20}O_3$ was determined based on the analysis of HR-ESI-MS data showing m/z peak at 249.1496 $[M + H]^+$ (calcd. for $C_{15}H_{20}O_3H$: 249.1412) (Fig. 1), and the analysis of ^1H NMR and ^{13}C NMR data (Table 1, Fig. S1, 2). The ^1H-NMR spectrum of **1** (in $CDCl_3$) showed the following signals: two tertiary methyl groups at δ 0.89 (3H, s) and 1.83 (3H, t, J = 1.6 Hz), which were typical of CH_3-14 and CH_3-13 of eudesmanolides; together with one terminal double bond at δ 4.60 (1H, d, J = 1.6 Hz) and 4.88 (1H, d, J = 1.6 Hz) for H-15. The ^1H-NMR patterns of **1** were similar to those of the known compound **5** (atractylenolide II) [21], as stated in the Supplementary data. However, the ^1H-NMR spectrum of **1** was distinct from that of **5** because there was one more proton signal at δ 3.88 (1H, d, J = 3.6 Hz). Moreover, in ^{13}C-NMR spectrum, there was an additional carbon signal at δ 75.4. Taking the molecular formula into account, it was suggested that hydroxylation had taken place on one of the secondary carbons. Compared with **5**, H-8 signals of **1** notably shifted to lower fields, from δ 4.80 (1H, t, J = 6.4 Hz) to δ 4.98 (1H, d, J = 2.0 Hz). Therefore, it was supposed that a hydroxylation took place at C-9, resulting in increased chemical shift values of H-8 for an inductive effect. In the heteronuclear multiple bond

correlation (HMBC) spectrum, the long-range correlations from the carbon signal at δ 75.4 (C-9), to H-8 signals confirmed the hydroxyl group located at C-9 (Table 1, Fig. S3, S5). The coupling constants and the cross peak between H-9 and the signal at δ 4.98 (1H, d, J = 2.0 Hz) and δ 0.89 (3H, s), assigned to H-8 and CH_3-14, respectively, in NOESY spectrum confirmed that the H-9 was axial and β-oriented (Fig. S4, S6). Finally, the chemical structure of **1** is formed by adding an extra oxygen in comparison with **5**, and **1** was established as 9α-hydroxyatractylenolide, namely 9α-hydroxyeudesma-4(15),7(11)-dien-8α,12-olide. As far as we know, its spectroscopic data had not been reported before.

Comparing with previously published data, the other compounds were identified as atractylone (**2**) [22], 3β-acetoxyatractylon (**3**) [22], atractylenolide I (**4**) [23], atractylenolide II (**5**) [21], 8-epiasterolid (**6**) [24], atractylenolide III (**7**) [14], atractylenolide VII (**8**) [25], 8-epiatractylenolide III (**9**) [14], eudesm-4(15)-ene-7α,11-diol (**10**) [26], linoleic acid (**11**) [27], myristic acid (**12**) [27], 3-*O*-caffeoyl-1-methyquinic acid (**13**) [28], (2E,8E,10E)-tetradecatriene-4,6-diyne-1,14-diol (**14**) [29], 14-aceroxy-12-senecioyloxytetradeca-2E,8Z,10E-trien-4,6-diyn-1-ol (**15**) [30], isoscopoletin (**16**) [31], caffeic acid (**17**) [32], protocatechic acid (**18**) [33], 3-*O*-caffeoylquinic acid (**19**) [28], 4-*O*-caffeoylquinic acid (**20**) [34], 1,5-di-*O*-caffeoylquinic acid (**21**) [35], and nicotinic acid (**22**) [36] (Fig. 3).

Although we tried to evaluate the bioactivity of the isolated compounds, the amounts of compounds **1**, **3** and **20** were too small to determine their bioactivities. In addition, compound **2** was obtained in a sufficient amount, but further NMR analysis indicated changes in the compound. Thus, the remaining 18 compounds (excluding compounds **1**, **2**, **3**, and **20** were used to examine their bioactivity.

Inhibitory effect of compounds isolated from *A. macrocephala* on LPS-induced NO production in RAW264.7 and BV2 cells

The production of NO is catalyzed by the enzymatic activity of nitric oxide synthase (NOS), which converts L-arginine to NO and L-citrulline via the intermediate N-hydroxy-l-arginine [37, 38]. NO is known to play a key role in regulating the vascular, immune, and nervous systems [39]. In inflammatory conditions, the expression of NOS increases in various immune cells including macrophages, monocytes, microglia, dendritic cells, eosinophils, and neutrophils, resulting in the release of large amounts of NO [38]. Subsequently, the overproduction of NO leads to development of inflammatory disorders in the joints, gut, and lungs [38], neurodegenerative diseases including Alzheimer's disease, Parkinson's disease, multiple sclerosis [39], and cancer [40]. As inhibiting NO production could have a therapeutic effect on inflammatory diseases, we investigated whether the compounds isolated from *A. macrocephala* might inhibit the LPS-induced NO production in RAW264.7 macrophages and BV2 microglial cells.

First, we evaluated whether the compounds exerted a cytotoxic effect on RAW264.7 and BV2 cells. Cells were treated with 5, 10, 20, 40, and 80 μM of selected compounds for 24 h, and cell viability was measured by MTT assay. The compounds showed no cytotoxicity for any of the tested concentrations (data not shown). Therefore, the three highest concentrations (20, 40, and 80 μM) were used in the NO assay. Cells were pre-treated with 20, 40, and 80 μM of compounds for 3 h, and then stimulated with LPS

(1 μg/mL) for 24 h. Regarding RAW264.7 cells, most compounds inhibited the LPS-induced NO production, except for compounds **7** and **9**, with IC_{50} values in the 26.8–78.1 μM range. In BV2 cells, all the tested compounds suppressed NO production in a concentration-dependent manner. Compounds **4**, **5**, **6**, **16**, and **17**, showed an inhibitory effect higher than 50% within the used concentration range, with IC_{50} values of 26.0 ± 0.23, 46.8 ± 1.12, 37.4 ± 4.03, 58.5 ± 2.23, and 72.3 ± 3.35 μM, respectively (Table 2).

Inhibitory effect of compound 6 on LPS-induced PGE_2 production in RAW264.7 and BV2 cells

The result of NO inhibitory effect showed that compound **4** has the lowest IC_{50} value among the tested compounds, indicating that it has the highest inhibitory effect. Previous studies have reported that compound **4** has anti-inflammatory effects in RAW264.7 macrophages by inhibiting the activation of NF-κB and MAPK signaling pathways mediated through the cluster of differentiation 14 (CD14)/toll-like receptor 4 (TLR4) pathways [16]. This compound also showed neuroprotective effects through the suppression of NF-κB pathway and induction of heme oxygenase (HO)-1 protein in BV2 microglia cells and in 1-methyl-4-phenyl-1,2,3,6-tetrahydropyridine (MPTP)-induced C57BL6/J models, suggesting that compound **4** might be effective in treating Parkinson's disease [17]. Compound **6** was the second most effective compound for NO production in both RAW264.7 and BV2 cells; additional experiments were conducted and showed that this compound possesses anti-inflammatory properties (Table 2).

Similar to NO, prostaglandins play an important role in the inflammatory process. Arachidonic acid (AA) in the body is converted into prostaglandin H2 (PGH_2) by the action of cyclooxygenase (COX)-1 and 2 enzymes [41]. Then, PGH_2 acts as a substrate of specific isomerase and synthase enzymes to produce various prostanoids including PGE_2, PGI_2, PGD_2, $PGF_{2\alpha}$, and thromboxane A2 (TXA_2) [42]. PGE_2 reacts with four types of receptors (EP1–EP4), each with its distinct signal-transduction properties, and exerts diverse physiological functions [43]. In this investigation, RAW264.7 and BV2 cells were pre-treated with compound **6** for 3 h, followed by stimulation with LPS (1 μg/mL) for 24 h to examine whether it affected PGE_2 production. It was found that pre-treatment with compound **6** significantly inhibited the LPS-induced PGE_2 production in both RAW264.7 and BV2 cells (Fig. 4).

Inhibitory effect of compound 6 on LPS-induced production of pro-inflammatory cytokines in RAW264.7 and BV2 cells

Cytokines are small secreted proteins produced by every cell and regulate the immune responses [44]. They consist of six major families including ILs, chemokines, interferons, TNF, growth factors of hematopoiesis and transforming growth factor-β (TGF-β) members [45]. In particular, the pro-inflammatory cytokines including IL-1β, IL-6 and TNF-α are produced from activated macrophages or microglia, and are associated with the up-regulation of inflammatory responses [44]. Compound **4** (atractylenolide I), which is one of the isolated compounds, has been reported that this compound inhibited the production of TNF-α and IL-6 in LPS-stimulated RAW264.7 cell model [16]. Another investigation demonstrated that compound **4** inhibited the production of TNF-α, IL-6, and IL-1β in LPS-induced BV2 microglial cell model, and that of TNF-α in MPTP-induced mice model [17]. Based on the

above reports, we examined whether compound **6** suppressed the production of pro-inflammatory cytokines in LPS-induced RAW264.7 and BV2 cells. Both cells were pre-treated with compound **6** for 3 h, and then stimulated with LPS (1 μg/mL) for 24 h. At a concentration of 80 μM, compound **6** significantly suppressed the LPS-induced production of IL-1β, IL-6, and TNF-α in both RAW264.7 and BV2 cells (Fig. 5).

Inhibitory effect of compound 6 on LPS-induced iNOS and COX-2 expression in RAW264.7 and BV2 cells

NO is synthesized from the L-arginine via the enzymatic activity of NOS. There are three different isoforms of NOS including neuronal nNOS (NOS1), inducible iNOS (NOS2), and endothelial eNOS (NOS3) [46]. Each enzyme has its own physiological characteristics. nNOS is expressed in neurons, and has been reported to mediate the long-term regulation of synaptic transmission [47]. eNOS is released mainly by endothelial cells; as it promotes blood vessel expansion and controls blood pressure, the functional anomalies in eNOS lead to the development of cardiovascular diseases [47]. eNOS is also known to control cancer-related phenomena such as angiogenesis, apoptosis, invasion, and metastasis [48]. nNOS and eNOS are constitutive forms that continuously secrete low concentrations of NO, and thus maintain several physiological functions. However, since iNOS is inducible, its production is increased by bacterial LPS, cytokines, chemokines, and other stimuli such as stress [47, 49].

As mentioned above, COX is involved in the generation of PGE_2. There are two COX isoforms: COX-1 and COX-2. The former is a constitutive type that is expressed in most tissues and is associated with conducting normal physiological functions [50, 51]. On the other hand, COX-2 is an inducible form and is up-regulated through various inflammatory stimuli of cytokines, growth factors, tumor promotors, and bacterial LPS, which then increase the amount of PGE_2 produced [52]. Although both COX-1 and COX-2 are related to the production of PGE_2, the continuous suppression of COX-1 activity could lead to side effects such as gastrointestinal toxicity or mild bleeding diathesis [53]. Therefore, the selective inhibition of COX-2 is necessary to block inflammatory responses.

Compound **6** showed a significant inhibitory effect on the LPS-induced NO and PGE_2 production in RAW264.7 and BV2 cells. Therefore, we further investigated the effect of compound **6** on the expression of iNOS and COX-2 proteins induced by LPS in both cell lines. Cells were pre-treated with compound **6** for 3 h, and then stimulated with LPS (1 μg/mL) for 24 h. The degree of expression of iNOS and COX-2 proteins in the lysates was determined using Western blot analysis. The pre-treatment with compound **6** at concentrations of 40 and 80 μM suppressed the LPS-induced iNOS and COX-2 expression in both RAW264.7 and BV2 cells (Fig. 6).

Effect of compound 6 on the LPS-induced activation of NF-κB and MAPK signaling pathways

NF-κB is one of the main transcription factors that regulates gene expression and that is involved in the production of pro-inflammatory mediators [54], development of immune cells, cell cycle, proliferation, and cell death [55]. This family consists of five structurally related members, including RelA (p65), p50, p52, RelB, and c-Rel, and these subunits form at least 12 different homo- or heterodimers [56]. There are two different signaling pathways: canonical and non-canonical pathways. The canonical pathway mainly

regulates RelA (p65), p50, and c-Rel, and the non-canonical pathway predominantly activates p52 and RelB. Both pathways are important for regulating immune and inflammatory responses [54, 57]. Under basal conditions, NF-κB dimers are present in the cytoplasm with their inhibitory protein IκB. However, pro-inflammatory cytokines or LPS can induce the phosphorylation and degradation of IκB, releasing NF-κB dimers and inducing phosphorylation [58]. Then, NF-κB dimers translocate into the nucleus, bind to the κB binding site, and regulate the expression of inflammatory genes including inflammatory enzymes (iNOS, COX-2), cytokines, and adhesion molecules [59]. Previous studies demonstrated that compound **4** (atractylenolide I) inhibited the LPS-induced activation of NF-κB in RAW264.7 and BV2 cells [16, 17]. Therefore, we examined whether compound **6** suppressed the activation of NF-κB pathway in LPS-induced RAW264.7 and BV2 cells. Both cell lines were pre-treated with compound **6** for 3 h, and then stimulated with LPS (1 μg/mL) for 1 h. The pre-treatment with compound **6** inhibited the LPS-induced phosphorylation and degradation of IκB-α as well as the phosphorylation of p65 in both RAW264.7 and BV2 cells (Fig. 7).

MAPK cascades are groups of serine/threonine protein kinases and have an important role in the transduction of extracellular signals to various cellular responses including proliferation, stress responses, apoptosis, and immune defense [60]. In mammalian cells, MAPK cascades consist of three major types, including p38, ERK, and JNK MAPKs, and each kinase can be activated by many different upstream MAPK kinases (MAP2K), and MAPK kinase kinases (MAP3Ks) [61]. The phosphorylation of MAPKs has been shown to be related to the enhancement of inflammatory responses through the induction of the release of pro-inflammatory mediators [60, 62]. In a previous study, compound **4** (atractylenolide I) inhibited the LPS-induced phosphorylation of p38 and ERK MAPKs, and showed anti-inflammatory activity in RAW264.7 cells [16]. Therefore, we investigated whether compound **6** affects the LPS-induced activation of the MAPK pathways in RAW264.7 and BV2 cells. Both cell lines were pre-treated with compound 6 for 3 h, and then stimulated with LPS (1 μg/mL) for 30 min. The phosphorylation levels of p38, ERK, and JNK remarkably increased by LPS-stimulation. The pre-treatment with compound **6** did not inhibited the activation of all three MAPKs (Fig. 8). These data suggested that compound **6** regulated the inflammatory responses by inhibiting of the NF-κB signaling pathway, not MAPK pathways.

Conclusion

In the present study, we isolated 22 compounds including 1 new compound and 21 known compounds from the MeOH extract of dried rhizomes of *A. macrocephala*. Analysis of ^{1}H-NMR, ^{13}C-NMR, HMBC, and NOESY spectrum of compound **1**, and comparing with published data of compound **5** resulted in the establishment of compound **1** as 9α-hydroxyatractylenolide, which was formed by adding an extra oxygen in compound **5**. The chemical structures of other compounds were determined by comparison with published data. The result of the NO assay revealed that compound **6** was the second most effective compound in both RAW264.7 macrophages and BV2 microglia stimulated by LPS. Compound **6** inhibited the LPS-induced production of PGE_2, the expression of iNOS and COX-2 protein, and the

production of pro-inflammatory cytokines including IL-1β, IL-6, and TNF-α in both cell lines. These inhibitory effects were regulated by inactivation of NF-κB signaling pathway by treatment with compound **6**. These results suggest that compound **6** is a good candidate for the development of inflammatory disease therapies.

Declarations

Ethics approval and consent to participate

Not applicable

Consent for publication

Not applicable

Availability of data and materials

The datasets generated and analyzed during the current study are available from the corresponding author on reasonable request.

Competing interests

The authors indicated no potential conflicts of interest.

Funding

This research was funded by the “Cooperative Research Program for Agriculture Science & Technology Development” (Project No. PJ01420801) of the Rural Development Administration, Republic of Korea.

Author Contributions

Kim YC, An RB, and Oh H managed the research project, provided guidance and supervised the study. Jin HG and An RB contributed to the isolation of compounds, and the conduction of HPLC and NMR. Kim KW and Li J carried out the biological assays. Jin HG and Kim KW wrote the manuscript. Lee DY, Yoon DH, Jeong JT and Kim GS prepared the plant materials, and funded the research. All authors read and approved the final manuscript.

Acknowledgements

The authors thank the Rural Development Administration for their provision of plant materials and funding for this research.

References

1. Abarikwu, S.O. 2014. Kolaviron, a natural flavonoid from the seeds of *Garcinia kola*, reduces LPS-induced inflammation in macrophages by combined inhibition of IL-6 secretion, and inflammatory transcription factors, ERK1/2, NF-κB, p38, Akt, p-c-JUN and JNK. *Biochimica et Biophysica Acta* 1840: 2373-2381.
2. Bain, C.C., and Mowar, A.M. 2014. Macrophages in intestinal homeostasis and inflammation. *Immunological Review* 260: 102-117.
3. Liu, Y.C., Zou, X.B., Chai, Y.F., and Yao, Y.M. 2014. Macrophage polarization in inflammatory diseases. *International Journal of Biological Sciences* 10: 520-529.
4. Navarro, V., Sanchez-Mejias, E., Jimenez, S., Muñoz-Castro, C., Sanchez-Varo, R., Davila, J.C., Vizuete, M., Gutierrez, A., and Vitorica, J. 2018. Microglia in Alzheimer's Disease: Activated, dysfunctional or degenerative. *Frontiers in Aging Neuroscience* 10: 140.
5. Joe, E.H., Choi, D.J., An, J., Eun, J.H., Jou, I., and Park, S. 2018. Astrocytes, microglia, and Parkinson's disease. *Experimental Neurobiology* 27: 77-87.
6. Inoue, K. 2006. The function of microglia through purinergic receptors: neuropathic pain and cytokine release. *Pharmacology & Therapeutics* 109: 210-226.
7. Zhang, X., Li, N., Shao, H., Meng, Y., Wang, L., Wu, Q., Yao, Y., Li, J., Bian, J., Zhang, Y., and Deng, X. 2016. Methane limit LPS-induced NF-κB/MAPKs signal in macrophages and suppress immune response in mice by enhancing PI3K/AKT/GSK-3β-mediated IL-10 expression. *Scientific Reports* 6: 29359.
8. Subedi, L., Lee, J.H., Yumnam, S., Ji, E., and Kim, S.Y. 2019. Anti-inflammatory effect of sulforaphane on LPS-activated microglia potentially through JNK/AP-1/NF-κB inhibition and Nrf2/HO-1 activation. *Cells* 8: 194.
9. Ngkelo, A., Meja, K., Yeadon, M., Adcock, I., and Kirkham, P.A. 2012. LPS induced inflammatory responses in human peripheral blood mononuclear cells is mediated through NOX4 and Giα dependent PI-3kinase signalling. *Journal of Inflammation (London)* 9: 1.
10. Chen, Y., Ji, N., Pan, S., Zhang, Z., Wang, R., Qiu, Y., Jin, M., and Kong, D. 2017. Roburic acid suppresses NO and IL-6 production via targeting NF-κB and MAPK pathway in RAW264.7 cells. *Inflammation* 40: 1959-1966.
11. Cao, X., Jin, Y., Zhang, H., Yu, L., Bao, X., Li, F., and Xu, Y. 2018. The anti-inflammatory effects of 4-((5-Bromo-3-chloro-2-hydroxybenzyl)amino)-2-hydroxybenzoic acid in lipopolysaccharide-activated primary microglial cells. *Inflammation* 41: 530-540.
12. Hoang, L.S., Tran, M.H., Lee, J.S., Ngo, Q.M., Woo, M.H., and Min, B.S. 2016. Inflammatory Inhibitory Activity of Sesquiterpenoids from *Atractylodes macrocephala* Rhizomes. *Chemical and Pharmaceutical Bulletin (Tokyo)* 64: 507-511.
13. The State Pharmacopoeia Commission of P.R. China. 2005. *Pharmacopeia of People's Republic of China*. Beijing: Chemical Industry Press.
14. Li, Y., and Yang, X.W. 2014. New eudesmane-type sesquiterpenoids from the processed rhizomes of *Atractylodes macrocephala*. *Journal of Asian Natural Products Research* 16: 123-128.

15. Gu, S., Li, L., Huang, H., Wang, B., and Zhang, T. 2019. Antitumor, antiviral, and anti-Inflammatory efficacy of essential oils from *Atractylodes macrocephala* Koidz. produced with different processing methods. *Molecules* 24: 2956.
16. Ji, G., Chen, R., and Zheng, J. 2014. Atractylenolide I inhibits lipopolysaccharide-induced inflammatory responses via mitogen-activated protein kinase pathways in RAW264.7 cells. *Immunopharmacology and Immunotoxicology* 36: 420-425.
17. More, S., and Choi, D.K. 2017. Neuroprotective role of atractylenolide-I in an in vitro and in vivo model of Parkinson's disease. *Nutrients* 9: 451.
18. Cheng, Y., Chen, T., Yang, X., Xue, J., and Chen, J. 2019. Atractylon induces apoptosis and suppresses metastasis in hepatic cancer cells and inhibits growth *in vivo*. *Cancer Management and Research* 11: 5883-5894.
19. Li, J., Li, F., Xu, Y., Yang, W., Qu, L., Xiang, Q., Liu, C., and Li, D. 2013. Chemical composition and synergistic antioxidant activities of essential oils from *Atractylodes macrocephala* and *Astragalus membranaceus*. *Natural Product Communications* 8: 1321-1324.
20. Liu, J., Chen, X., Yue, C., Hou, R., Chen, J., Lu, Y., Li, X., Li, R., Liu, C., Gao, Z., Li, E., Li, Y., Wang, H., Yan, Y., Li, H., and Hu, Y. 2015. Effect of selenylation modification on immune-enhancing activity of *Atractylodes macrocephala* polysaccharide. *International Journal of Biological Macromolecules* 72: 1435-1440.
21. Li, Y., Liu, J., and Yang, X.W. 2013. Four new eudesmane-type sesquiterpenoid lactones from atractylenolide II by biotransformation of rat hepatic microsomes. *Journal of Asian Natural Products Research* 15: 344–356.
22. Yoichi, N., Yohya, W., Takako, S., and Seto, T. 1976. Studies on the components of atractylodes. I. New sewquiterpwnoids in the rhizome of *Artactylodes lancea* De candolle. *Yakugaku Zasshi* 96: 1089-1093.
23. Li, Y., and Yang, X.W. 2013. Five new eudesmane-type sesquiterpenoid lactones biotransformed from atractylenolide I by rat hepatic microsomes. *Fitoterapia* 85: 95-100.
24. Chen, L.G., Jan, Y.S., Tsai, P.W., Norimoto, H., Michihara, S., Murayama, C., and Wang, C.C. 2016. Anti-inflammatory and anti-nociceptive constituents of *Atractylodes japonica* Koidzumi. *Journal of Agricultural and Food Chemistry* 64: 2254-2262.
25. Ding, H.Y., Liu, M.Y., Chang, W.L., and Lin, H.C. 2005. New sesquiterpenoids from the rhizomes of *Atractylodes macrocephala*. *Chinese Pharmaceutical Journal* 57: 37-42.
26. Wang, H.X., Liu, C.M., Liu, Q., and Gao, K. 2008. Three types of sesquiterpenes from rhizomes of *Atractylodes lancea*. *Phytochemistry* 69: 2088–2094.
27. Guo, H., Diao, Q.P., Zhang, B., Wang, W.F., and Wang, L.X. 2018. Chemical constituents from *Pholiota nameko*. *Journal of Chinese Medicinal Materials* 41: 350–352.
28. Kamto, E.L.D., Ngono, D.S.B., Mbing, J.N., Atchadé, A.D.T., Pegnyemb, D.E., and Westhuizen, J.H.V.D. 2014. An aromatic amide C-glycoside and a cyclitol derivative from stem barks of *Piper guineense* Schum and Thonn (Piperaceae). *Phytochemistry Letters* 10: lxxvi-lxxxi.

29. Ruth, J., Ferdinand, B., and Siegmar, S. 1979. Weitere acetylenverbindungen aus Centaurea ruthenica. *Phytochemistry* 18: 829-837.
30. Chen, Z.L. 1987. The acetylenes from *Atractylodes macrocephala*. *Planta Medica* 53: 493–494.
31. Jerezano, A., Jiménez, F., Cruz, M.C., Montiel, L.E., Delgado, F., and Tamariz, J. 2011. New approach for the construction of the coumarin frame and application in the total synthesis of natural products. *Hevetica Chimica Acta* 94: 185-198.
32. Zhu, T.F., Chen, J.J., Sun, Q.W., and Yan, Z.H. 2017. Chemical constituents from *Picrorhiza scrophulariiflora*. *Chinese Traditional and Herbal Drugs* 48: 263–265.
33. Xiao, S.J., Guo, D.L., He, D.H., Xia, B., Chen, F., Ding, L.S., and Zhou, Y. 2016. Chemical constituents of *Clematoclethra scandens* subsp. actinidioides. *Chinese Traditional and Herbal Drugs* 47: 383–387.
34. Nakatani, N., Kayano, S., Kikuzaki, H., Sumino, K., Katagiri, K., and Mitani, T. 2000. Identification, quantitative determination, and antioxidative activities of chlorogenic acid isomers in prune (*Prunus domestica* L.). *Journal of Agricultural and Food Chemistry* 48: 5512-5516.
35. Carnat, A., Heitz, A., Fraisse, D., Carnat, A.P., and Lamaison, J.L. 2000. Major dicaffeoylquinic acids from Artemisia vulgaris. *Fitoterapia* 71: 587-589.
36. Ma, H.Y., Sun, Y., Lu, A.L., Chen, G., Wu, H.H., and Pei, Y.H. 2010. Isolation and identification of chemical constituents from *Artemisia capillaries* Thunb. *Chinese Journal of Medicinal Chemistry* 20: 61–63.
37. Shih, R.H., Wang, C.Y., and Yang, C.M. 2015. NF-kappaB signaling pathways in neurological inflammation: A mini review. *Frontiers in Molecular Neuroscience* 8: 77.
38. Liu, Y., Shepherd, E.G., and Nelin, L.D. 2007. MAPK phosphatases-Regulating the immune response. *Nature Reviews Immunology* 7: 202-212.
39. Coleman, J.W. 2001. Nitric oxide in immunity and inflammation. *International Immunopharmacology* 1: 1397-1406.
40. Sharma, J.N., Al-Omran, A., and Parvathy, S.S. 2007. Role of nitric oxide in inflammatory diseases. *Inflammopharmacology* 15: 252-259.
41. Guix, F.X., Uribesalgo, I., Coma, M., and Muñoz, F.J. 2005. The physiology and pathophysiology of nitric oxide in the brain. *Progress in Neurobiology* 76: 126-152.
42. Choudhari, S.K., Chaudhary, M., Bagde, S., Gadbail, A.R., and Joshi, V. 2013. Nitric oxide and cancer: a review. *World Journal of Surgical Oncology* 11: 118.
43. Andreasson, K. 2010. Emerging roles of PGE_2 receptors in models of neurological disease. *Prostaglandins & Other Lipid Mediators* 91: 104-112.
44. Ricciotti, E., and FitzGerald, G.A. 2011. Prostaglandins and inflammation. *Arteriosclerosis, Thrombosis, and Vascular Biology* 31: 986-1000.
45. Kawahara, K., Hohjoh, H., Inazumi, T., Tsuchiya, S., and Sugimoto, Y. 2015. Prostaglandin E2-induced inflammation: Relevance of prostaglandin E receptors. Biochimica et Biophysica Acta 1851: 414-421.

46. Blantz, R.C., and Munger, K. 2002. Role of nitric oxide in inflammatory conditions. *Nephron* 90: 373-378.
47. Förstermann, U., and Sessa, W.C. 2012. Nitric oxide synthases: regulation and function. *European Heart Journal* 2012, 33: 829-837.
48. Ying, L., and Hofseth, L.J. 2007. An emerging role for endothelial nitric oxide synthase in chronic inflammation and cancer. *Cancer Research* 67: 1407-1410.
49. Wu, X., Gao, H., Sun, W., Yu, J., Hu, H., Xu, Q., and Chen, X. 2017. Nepetoidin B, a natural product, inhibits LPS-stimulated nitric oxide production via modulation of iNOS mediated by NF-κB/MKP-5 pathways. *Phytotherapy Research* 31: 1072-1077.
50. Sales, K.J., and Jabbour, H.N. 2003. Cyclooxygenase enzymes and prostaglandins in pathology of the endometrium. *Reproduction* 126: 559-567.
51. Williams, C.S., Mann, M., and DuBois, R.N. 1999. The role of cyclooxygenases in inflammation, cancer, and development. *Oncogene* 18: 7908-7916.
52. Morita, I. 2002. Distinct functions of COX-1 and COX-2. *Prostaglandins & Other Lipid Mediators* 68-69: 165-175.
53. Simon, L.S. 1999. Role and regulation of cyclooxygenase-2 during inflammation. *The American Journal of Medicine* 106: 37S-42S.
54. Zhang, J.M., and An, J. 2007. Cytokines, Inflammation, and Pain. *International Anesthesiology Clinics* 45: 27-37.
55. Kuspa, T., Horacek, J.M., and Jebavy, L. 2012. The Role of Cytokines in Acute Myeloid Leukemia: A Systematic Review. *Biomedical Papers of the Medicinal Faculty of the University Palacky, Olomouc, Czechoslovakia* 156:291-301.
56. Liu, T., Zhang, L, Joo, D., and Sun, S.C. 2017. NF-κB Signaling in inflammation. *Signal Transduction and Targeted Therapy* 2: 17023.
57. Christian, F., Smith, E.L., and Carmody, R.J. 2016. The regulation of NF-κB subunits by phosphorylation. *Cells* 5: 12.
58. Giridharan, S., and Srinivasan, M. 2018. Mechanisms of NF-κB p65 and strategies for therapeutic manipulation. *Journal of Inflammation Research* 11, 407-419.
59. Lawrence, T. 2009. The Nuclear Factor NF-kappaB Pathway in Inflammation. *Cold Spring Harbor Perspectives in Biology* 1: a001651.3
60. Viatour, P., Merville, M.P., Bours, V., and Chariot, A. 2005. Phosphorylation of NF-kappaB and IkappaB proteins: Implications in cancer and inflammation. *Trends in Biochemical Sciences* 30: 43-52.
61. Kyriakis, J.M., and Avruch, J. 2012. Mammalian MAPK signal transduction pathways activated by stress and inflammation: A 10-year Update. *Physiological Reviews* 92: 689-737.
62. Ci, X., Ren, R., Xu, K., Li, H., Yu, Q., Song, Y., Wang, D., Li, R., and Deng, X. 2010. Schisantherin A exhibits anti-inflammatory properties by down-regulating NF-kappaB and MAPK signaling pathways in lipopolysaccharide-treated RAW 264.7 Cells. *Inflammation* 33: 126-136.

Tables

Table 1. NMR data for compound 1 in $CDCl_3$

No	δC[a]	δH (*J*, Hz)[b]	HMBC
1	34.6	1.33 (1H, m)	
		2.06 (1H, dd, *J* = 13.6, 4.4 Hz)	C_2, C_{10}, C_{14}
2	22.3	1.60 (2H, m)	
3	36.3	1.96 (1H, m)	C_2, C_4, C_{15}
		2.35 (1H, m)	C_4
4	148.9		
5	42.2	2.38 (1H, m)	C_{10}
6	25.6	2.31 (1H, m)	C_7, C_{10}
		2.67 (1H, dq, *J* = 12.8, 3.2 Hz)	C_7, C_8, C_{10}
7	159.1		
8	79.9	4.98 (1H, d, *J* = 2.0 Hz)	
9	75.4	3.88 (1H, d, *J* = 3.6 Hz)	C_5, C_7, C_8
10	41.0		
11	121.9		
12	175.1		
13	8.4	1.83 (3H, t, *J* = 1.6 Hz)	C_7, C_{11}, C_{12}
14	15.7	0.89 (3H, s)	C_1, C_5, C_9, C_{10}
15	107.3	4.88 (1H, d, *J* = 1.6 Hz)	C_3, C_5
		4.60 (1H, d, *J* = 1.6 Hz)	

Table 2. Inhibitory effects of the test compounds on LPS-induced NO production in RAW264.7 and BV2 cells.

Compounds	RAW264.7	BV2
4	26.8 ± 3.86	26.0 ± 0.23
5	60.5 ± 16.8	46.8 ±1.12
6	39.1 ± 3.22	37.4 ± 4.03
7	1.7% at 80 μM	20.3% at 80 μM
8	50.8 ± 7.38	35.9% at 80 μM
9	9.2% at 80 μM	27.3% at 80 μM
10	64.3 ± 12.1	24.2% at 80 μM
11	41.2 ± 4.97	47.7% at 80 μM
12	36.7 ± 4.11	35.9% at 80 μM
13	59.2 ± 14.9	25.0% at 80 μM
14	28.4 ± 6.55	29.7% at 80 μM
15	51.3 ± 7.28	38.9% at 80 μM
16	29.8 ± 2.52	58.5 ± 2.23
17	34.8 ± 2.54	72.3 ± 3.35
18	44.5 ± 4.34	41.7% at 80 μM
19	28.8 ± 3.09	45.8 % at 80 μM
21	78.1 ± 23.5	36.7% at 80 μM
22	28.0 ± 2.94	47.2% at 80 μM

Figures

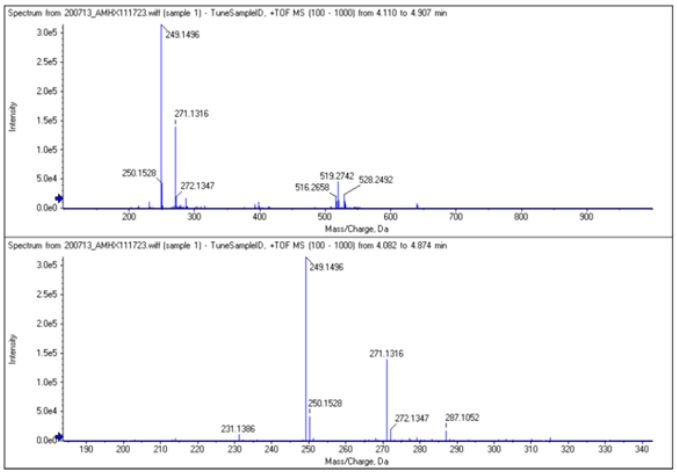

Fig. 1.

Figure 1

HR-ESI-MS spectrum of compound 1.

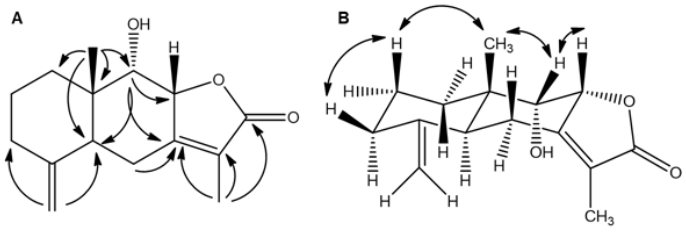

Fig. 2.

Figure 2

The key HMBC (A) and NOESY (B) correlations (arrow) of compound 1.

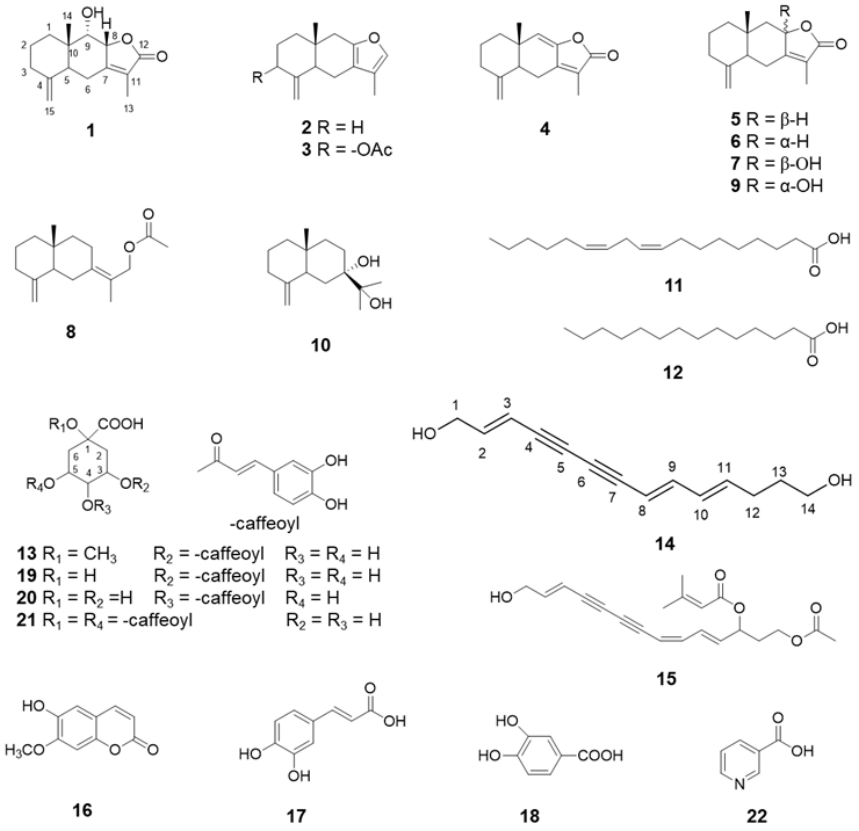

Fig. 3.

Figure 3

The chemical structures of compounds 1-22 isolated from Atractylodes macrocephala.

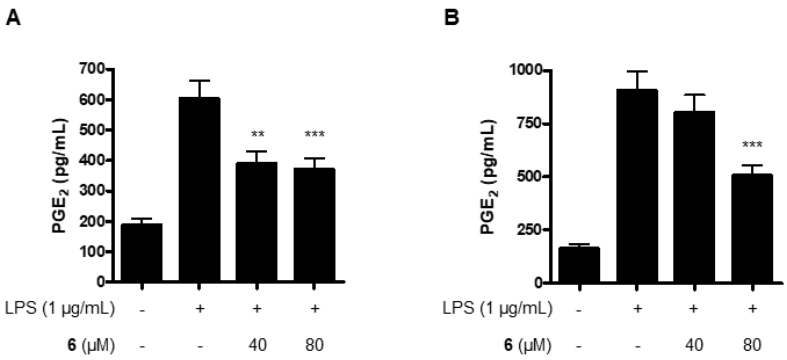

Fig. 4.

Figure 4

The effect of compound 6 on the LPS-induced production of PGE2 in RAW264.7 (A) and BV2 cells (B). Cells were pre-treated with or without the indicated concentrations of compound 6 for 3 h, and then stimulated with LPS (1 μg/mL) for 24 h. The level of PGE2 was quantified by ELISA. Values shown are means ± SD of three independent experiments. Experimental data are considered statistically significant at values. **p < 0.01 and ***p < 0.001 in comparison with the LPS group.

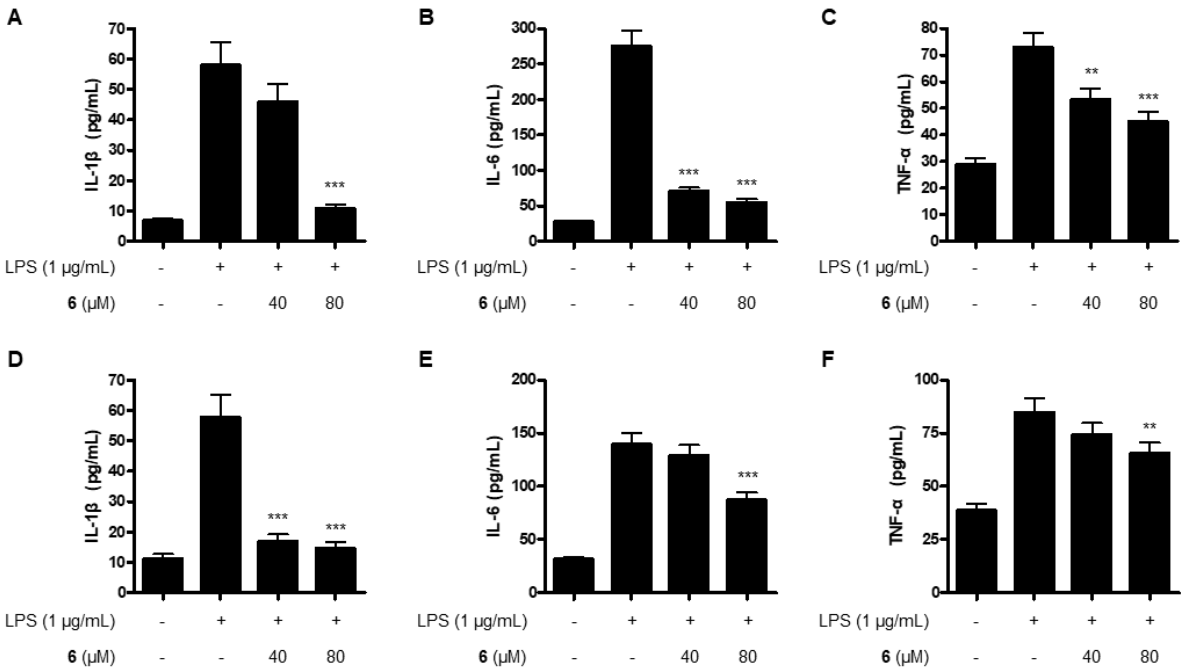

Fig. 5.

Figure 5

The effect of compound 6 on the LPS-induced production of pro-inflammatory cytokines in RAW264.7 (A, B, C) and BV2 cells (D, E, F). Cells were pre-treated with or without the indicated concentrations of compound 6 for 3 h, and then stimulated with LPS (1 μg/mL) for 24 h. The levels of pro-inflammatory cytokines were quantified by ELISA. Values are shown as mean ± SD of three independent experiments. Experimental data are considered statistically significant at values. **$p < 0.01$ and ***$p < 0.001$ in comparison with the LPS group.

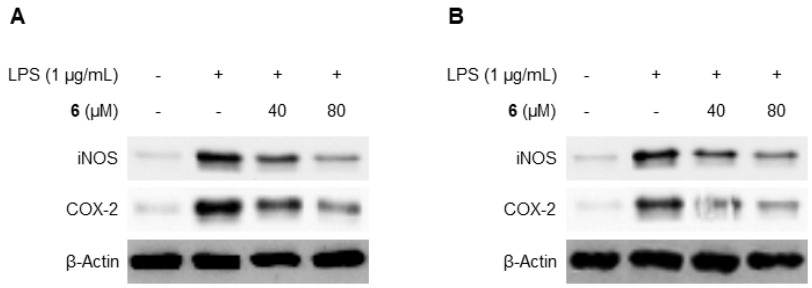

Fig. 6.

Figure 6

The effect of compound 6 on the LPS-induced expression of iNOS and COX-2 protein in RAW264.7 (A) and BV2 cells (B). Lysates were prepared from cells pre-treated with or without the indicated concentrations of compound 6 for 3 h and then with LPS (1 μg/mL) for 24 h. The level of expression of iNOS and COX-2 proteins was determined by Western blot analysis. Representative blots from three independent experiments are shown.

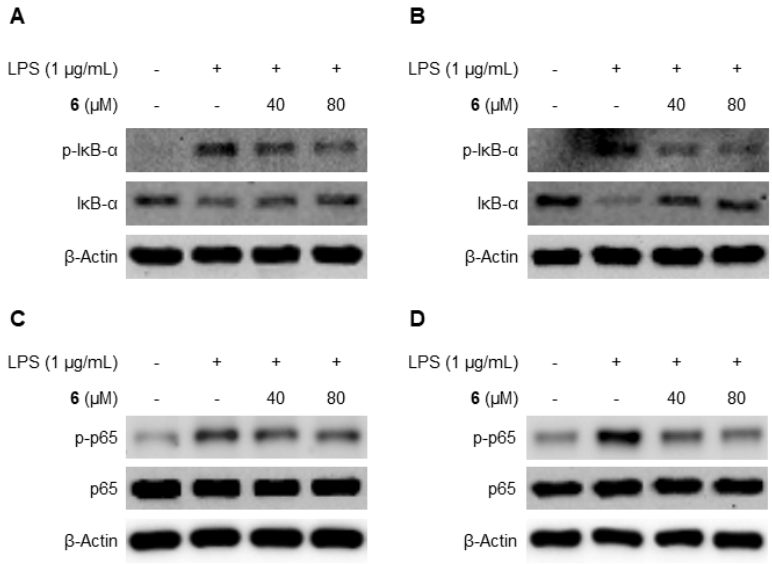

Fig. 7.

Figure 7

The effect of compound 6 on the LPS-induced activation of NF-κB pathway in RAW264.7 (A, C) and BV2 cells (B, D). Lysates were prepared from cells pre-treated with or without the indicated concentrations of compound 6 for 3 h and then with LPS (1 μg/mL) for 1 h. The level of expression of proteins was determined by Western blot analysis. Representative blots from three independent experiments are shown.

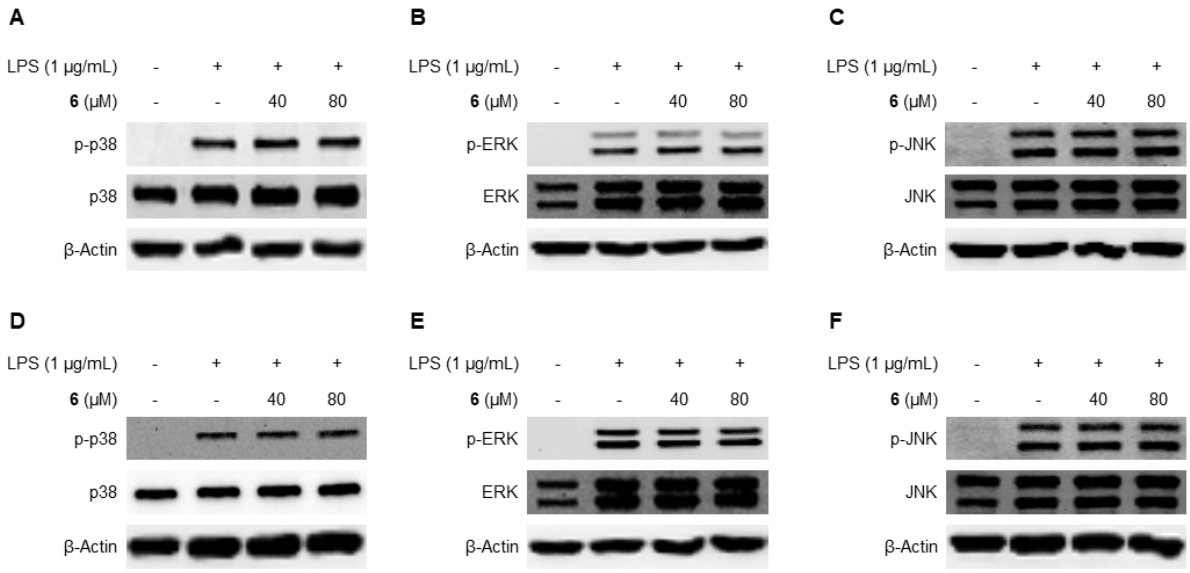

Fig. 8.

Figure 8

The effect of compound 6 on the LPS-induced activation of MAPK cascades in RAW264.7 (A, B, C) and BV2 cells (D, E, F). Lysates were prepared from cells pre-treated with or without the indicated concentrations of compound 6 for 3 h and then with LPS (1 μg/mL) for 30 min. The expression level of proteins was determined by Western blot analysis. Representative blots from three independent experiments are shown.

Supplementary Files

This is a list of supplementary files associated with this preprint. Click to download.

- AMSupplementaryMaterialsInflammation.docx